EPSC2026-1214 (TP16)

Developing a numerical model of photo-emitted electron energy spectra and its applications

Contact: Masahisa Kato (katomasa@rs.tus.ac.jp)

M. Kato[1], Y. Harada[2], S. Xu[3], A R. Poppe[3], and J. S. Halekas[4] ,Y. Saito[5], M. N. Nishino[5], S. Yokota[6], F. Takahashi[7], H. Shimizu[8]

1: Tokyo University of Science, Japan, 2: Nagoya University, Japan, 3: University of California, Berkeley, US, 4: University of Iowa, US, 5: Japan Aerospace Exploration Agency, Japan, 6: Osaka University, Japan, 7: Kyushu University, Japan, 8: The University of Tokyo, Japan

Key points

- We developed a numerical model of the energy spectra of photoelectrons emitted from the sunlit lunar surface.
- Model-observation comparisons reveal spatial and temporal variations in the lunar surface potential.
- Our numerical model can be applied to evaluate the plasma environment near the surface of the Moon and other airless bodies.

1. Introduction

Charged particle environment on the lunar surface

Since the Moon lacks a dense atmosphere and a global magnetic field, the lunar surface interacts directly with ambient charged particles.
As a result of the interaction, the lunar surface potential varies to balance incoming and outgoing electric currents driven by the charged particles (Manka, 1974; Fig. 1).

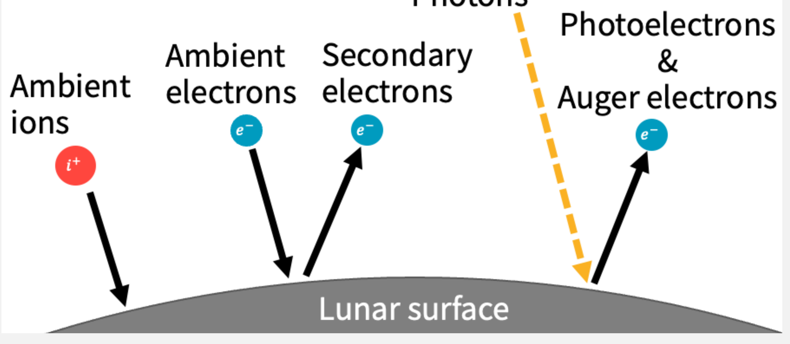

Fig. 1
Schematic illustration of the charged particle environment on the lunar surface.

Characteristics of photo-emitted electrons and the dayside surface potential

On the dayside, photoelectrons are emitted from the surface, and Auger electrons, which have characteristic energies that depend on the source atoms, are also emitted in response to photoemission (*e.g.*, Xu *et al.*, 2021; Fig. 2).
Because photoemission dominates the current balance, the dayside lunar surface potential tends to be positive (*e.g.*, Stubbs *et al.*, 2014). However, the potential varies depending on the ambient plasma environment (*e.g.*, Halekas *et al.*, 2008, 2011; Poppe *et al.*, 2011, 2012, 2015), crustal magnetic anomalies (Burke *et al.*, 1975; Futaana *et al.*, 2013), and solar activity (Sternovsky *et al.*, 2008).

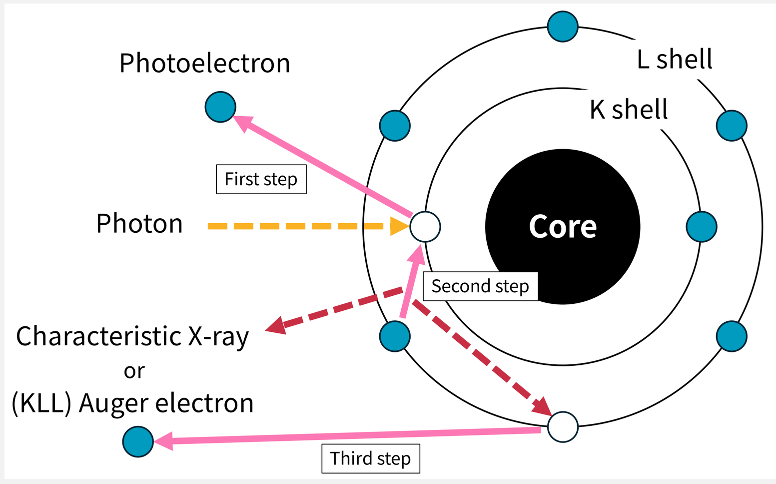

Fig. 2
Schematic illustration of the Auger electron emission process.

In this study, we use a numerical model of photoemitted electron energy spectra from the dayside lunar surface (Kato *et al.*, 2023) to investigate the dayside surface potential variability based on model-observation comparisons.

2. Methods

Numerical model (Kato *et al.*, 2023)

Input	Parameters	Output (Fig. 3)
FISM2, Energy spectra of solar irradiation model (Chamberlin et al., 2020)	Physical and chemical parameters related to photoemission (*e.g.*, Photoionization cross sections)	Energy spectra of photo-emitted electrons (photoelectrons and Auger electrons)

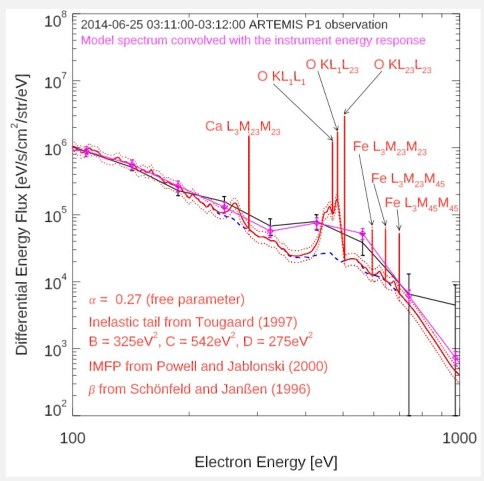

Fig. 3
Representative energy spectra observed by THEMIS-ARTEMIS (black), detailed model spectra (red), and an estimated observation (magenta) (Kato *et al.*, 2023).

Estimating the surface potential by model-observation comparison

By comparing model calculations with the electron observations from Kaguya and THEMIS-ARTEMIS above the lunar surface, we can estimate the potential difference between the spacecraft and the surface from the relative energy shift of photo-emitted electrons (Fig. 4).
When the spacecraft potential is known as is the case for ARTEMIS, we can also estimate the lunar surface potential.

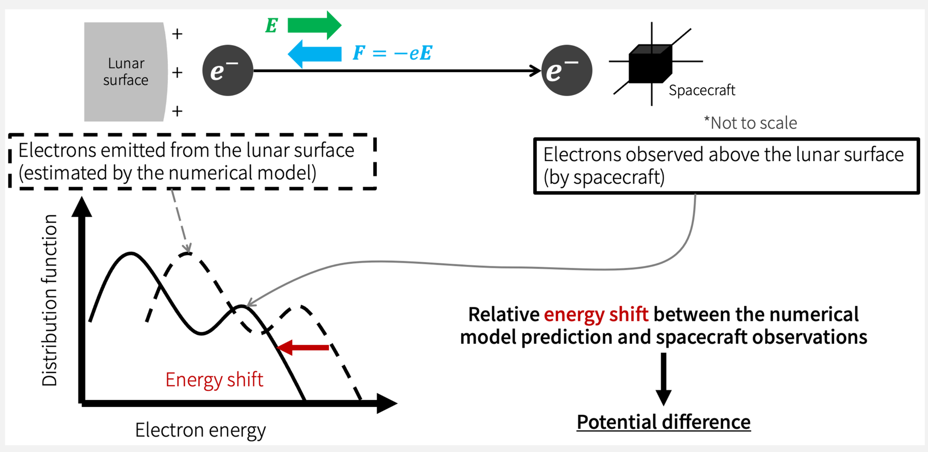

Fig. 4
Schematic diagram illustrating the estimation of the potential difference between the lunar surface and the spacecraft by model-observation comparison.

3. Results and discussion of model applications

3.1. Relationship between surface potential and potential minimum above the surface

Non-monotonic potential distributions can form above the lunar surface (Fig. 4), as indicated by upward-accelerated electron beams above the dayside lunar surface (Poppe *et al.*, 2012; Fig. 5).
Our event study based on model-observation comparison shows that the minimum potential and the surface potential vary synchronously (Kato *et al.*, 2023; Fig. 6).
Future studies should investigate the controlling factors of these potentials and the threshold between monotonic and non-monotonic potential distributions.

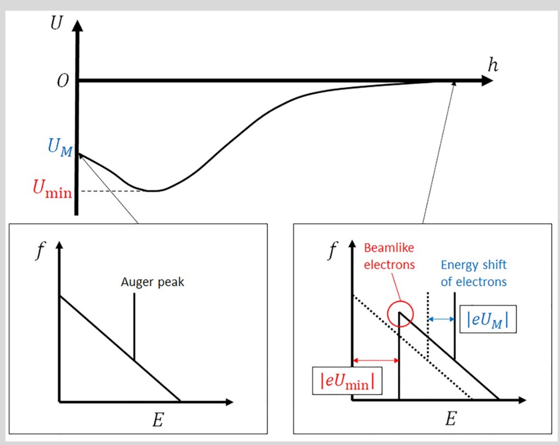

Fig. 4
Schematic illustration of non-monotonic potential distribution (Kato *et al.*, 2023).

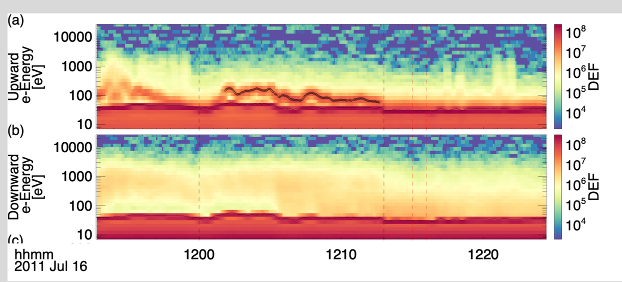

Fig. 5
Representative observations of upward electron beams above the dayside lunar surface (modified from Kato et al. (2023)).

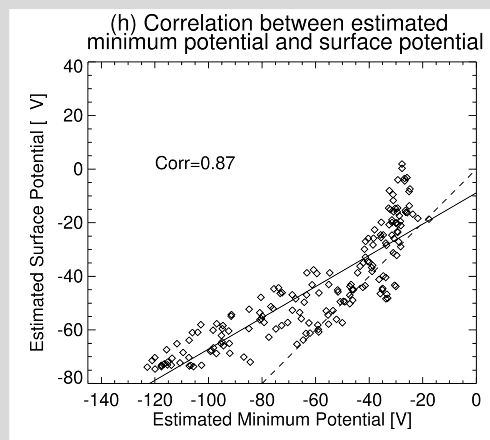

Fig. 6
Relationship between potential minimum and surface potential on July 16, 2011 (modified from Kato *et al.* (2023)).

3.2. Relationship between surface potential and crustal magnetized regions

Our analysis using Kaguya observations shows that electrons originating from magnetized regions are more strongly decelerated than those from non-magnetized regions, corresponding to a more positive surface potential over magnetized regions in the lobes (Kato *et al.*, 2025).
Although a more positive potential is expected over magnetized regions, consistent with previous studies in the solar wind (Futaana *et al.*, 2013) and plasma sheet (Burke *et al.*, 1975), the energy shift is smaller than in those studies.

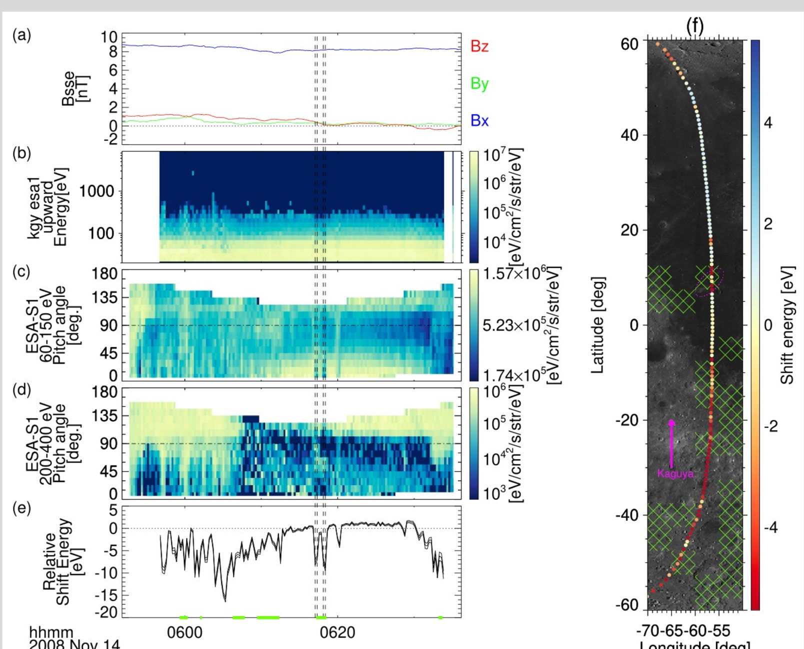

Fig. 7
Electron observations and estimated energy shift of emitted electron observations (Kato *et al.*, 2025).

3.3. Relationship between surface potential and solar activity

We evaluate variations in photon emission associated with solar activity using the FISM2 model (Chamberlin *et al.*, 2020).
Considering the current balance between downgoing electrons observed by ARTEMIS and upgoing electrons calculated by the model, we find that the surface potential becomes more positive as solar activity increases and it can exceed +100 V in the lobes during solar flares (Kato *et al.*, 2026).

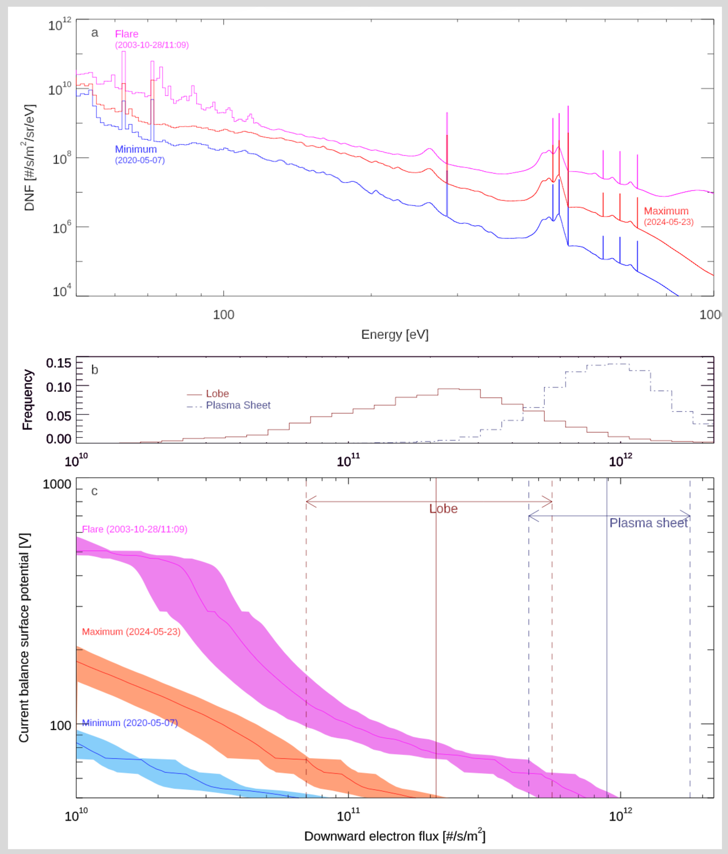

Fig. 8
Calculated photo-emitted electron energy spectra and estimation of the current balance potential for different solar activity (Kato *et al.*, 2026)

References

Burke, W. J. et al. (1975), Proc. Lunar Sci. Conf. 6th p. 2985-2997
Chamberlin, P. C. et al. (2020), Space Weather, 18, e2020SW002588
Futaana, Y., et al. (2013), Geophys. Res. Lett., 40, 262-266
Halekas, J. S. et al. (2008), J. Geophys. Res., 113, A09102
Halekas, J. S. et al. (2011), J. Geophys. Res., 116, A07103
Kato, M. et al. (2023), J. Geophys. Res.: Space Phys., 128, e2023JA031707
Kato, M. et al. (2025), J. Geophys. Res.: Space Phys., 130, e2024JA033545
Kato, M. et al. (2026), Geophys. Res. Lett., 53, e2025GL120581
Manka, R. (1973), Photon and Particle Interactions with Surfaces in Space, 347-361
Poppe, A. R. et al. (2011), Geophys. Res. Lett., 38, L02103
Poppe, A. R. et al. (2012), Geophys. Res. Lett., 39, L01102
Poppe, A. R. et al. (2015), Planet. Space Sci., 119, 111-120
Sternovsky, Z. et al. (2008), J. Geophys. Res., 113, A10104
Stubbs, T. J. et al. (2014), Planet. Space Sci. 90, 10-27